

Optical Studies of Inertially Confined Molecular Iodine Ions

D. T. Strickland, Y. Beaudoin, P. Dietrich, and P. B. Corkum

Steacie Institute for Molecular Sciences, National Research Council of Canada, Ottawa, Ontario, Canada K1A 0R6
(Received 30 September 1991)

We observe the kinetic energy of ionic fragments that result from the Coulomb explosion of molecular iodine ions produced by rapid multiphoton ionization. Because the ion energies produce a clear signature of the molecular ion state from which they originate, we are able to determine the intensity dependence of the molecular multiphoton ionization. Generalizations of atomiclike concepts are used to model the experimental results. Measurements of angular distributions indicate the importance of the molecular polarizability.

PACS numbers: 33.80.Gj, 33.80.Wz

We report optically driven molecular explosions in which the molecule is ionized to a highly charged state before there is significant motion of the constituent ions. We accomplish this by using an ultrashort pulse and I_2 , a weakly bound, heavy molecule with a ground-state vibrational period of 155 fs and a rotational period of $500/J$ ps, where J is the rotational quantum number. The resulting atomic ions have the characteristic kinetic energies of the different decay paths of the highly charged molecular ions.

Using the ion kinetic energy as a spectroscopic monitor of the ionization state of a molecular ion, we make the first quantitative measurements of the intensity dependence of the ionization rates due to nonresonant multiphoton ionization of a highly charged molecule. Although many experiments have studied aspects of strong-field interactions with molecular ions [1], previous studies of highly charged ions have been hampered because dissociation occurs during the duration of the laser pulse. In contrast, ionization of atomic ions has been extensively and quantitatively studied during the last decade [2].

The experiment uses a 630-nm pulse with either an 80-fs pulse or a 30-fs duration [3]. The near diffraction-limited pulses were focused into the target chamber with either an $F/2$ or an $F/20$ on-axis parabolic mirror. 3×10^{-6} Torr of iodine was leaked into the vacuum chamber. The fragment ions were diagnosed in a time-of-flight mass spectrometer with accelerating electrodes separated by 17 mm (Fig. 1) and 30 mm (Figs. 2 and 3) and maintained at a potential difference, which could be varied. A field-free drift region of 49 mm (Fig. 1) or 32 mm (Figs. 2 and 3) was terminated by an electrode containing a 2-mm-diam hole to select those ions with only a small velocity component transverse to the drift axis of the tube. The ion current was registered on a microchannel plate.

Figure 1(a) shows the I^+ component of the time-of-flight spectrum obtained by analysis of approximately 50 shots. The 30-fs pulse was used for these measurements. A number of features can be identified. At times corresponding to low kinetic energies [about $0.5 \mu\text{s}$ in Fig. 1(a)] we see a complex time-of-flight spectrum. This structure comes from the dissociation of I_2^{2+} into an ion and a neutral atom. It indicates that the molecule is left in repulsive electronic states at the end of the pulse.

There are three other distinct features of the spectrum, each having time shifts (with respect to the drift time of a zero initial kinetic-energy ion) characteristic of the explosion of I_2^{2+} , I_2^{3+} , and I_2^{4+} [peaks labeled 1+1, 1+2, and 1+3 in Fig. 1(a)]. In all cases, the spectra have a peak shift approximately given by the Coulomb energy at the ground-state internuclear separation of 2.66 Å. Even with the electrostatic force expected for I_2^{4+} decaying

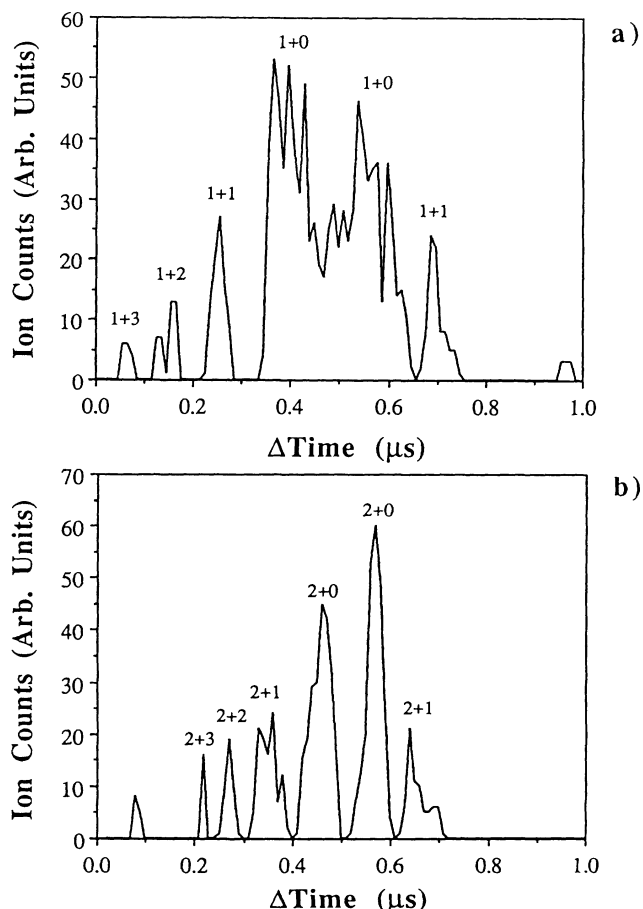


FIG. 1. Time-of-flight mass spectra of (a) I^+ and (b) I_2^{2+} showing transit times characteristic of the explosions of different charged states of I_2 . The various decay paths are labeled. Because of the construction of the time-of-flight chamber, channels do not occur symmetrically about the position of the zero-kinetic-energy ion.

TABLE I. Tabulation of the decay pathways with their associated field-free ionization potential V_m and effective ionization potential $V_{\text{eff}}(E_e)$. Also tabulated are relative experimental intensities I_{expt} obtained from Fig. 3 using an ion signal of 100 arbitrary units and the threshold intensity calculated using the barrier suppression model I_b in relative units; absolute units are obtained by multiplying with 0.8×10^{13} or 3×10^{13} W/cm², respectively.

$I_2 \rightarrow I_2^{n+} \rightarrow$	$V_m(0)$ (eV)	$V_{\text{eff}}(E_e)$ (eV)	I_{expt} (8×10^{12} W cm ⁻²)	I_b (3×10^{13} W cm ⁻²)
$I_2^+ = I^+ + I^0$	9.3	9.3	1.0	1.0
$I_2^{2+} = I^+ + I^+$	18.5	16.9	3.1	2.7
$I_2^{2+} = I^{2+} + I^0$	16.4	16.4	3.7	2.4
$Xe \rightarrow Xe^+$	12.1	12.1	4.1	2.9
$I_2^{3+} = I^{2+} + I^+$	26.5	24.7	5.8	4.3
$I_2^{3+} = I^{3+} + I^0$	38.4	38.4	Not observed	32.3
$Xe^+ \rightarrow Xe^{2+}$	21.2	21.2	16	6.7
$I_2^{4+} = I^{2+} + I^{2+}$	29.9	26.4	10	4.9
$I_2^{4+} = I^{3+} + I^+$	38.4	36.1	17	14.8
$I_2^{5+} = I^{3+} + I^{2+}$	43.8	40.2	16	14.7
$I_2^{5+} = I^{4+} + I^+$	49.5	47.8	Not observed	26.8
$I_2^{6+} = I^{3+} + I^{3+}$	49.2	55.2	31	34.0
$I_2^{6+} = I^{4+} + I^{2+}$	54.8	50.7	Observed but not measured	25.9

into $I^{3+} + I^+$, we expect ion motion of only 0.2 Å in 30 fs, corresponding to a potential difference of about 0.5 eV per ion. We have confirmed this conclusion experimentally by investigating multiphoton ionization with a 70-fs pulse.

The appearance of a decay channel with kinetic energy characteristic of the asymmetric explosion of I_2^{4+} is a significant observation. Asymmetric decay has been suggested previously for long-pulse experiments [4] (laser pulses much longer than the explosion time) but it has been a subject of considerable controversy [5]. Figure 1 unambiguously shows that these charge-asymmetric molecular states are produced in significant quantities in inertially confined molecules, either in the excitation process (excited electronic states are populated that lead to unequally charged products) or in the field-free dissociation (avoided crossings) process. We show in Table I that the data are consistent with significant, direct laser excitation of asymmetric states. This result should not be a surprise. In a classic paper, Mulliken [6] showed that states which lead to asymmetric decay products are very strongly coupled to the symmetric states by charge-transfer transitions.

Figure 1(b) shows the I_2^{2+} decay channel. The central component corresponds to ions with energy much less than the Coulomb decay energy of any molecular ion of charge greater than 2. It results from the decay of I_2^{2+} into $I^{2+} + I$. All other decay channels containing I^{2+} , up to I_2^{5+} , are observed at their characteristic Coulomb explosion energy, slightly broadened to the low-energy side. Similar spectra are obtained for the I_2^{3+} . The ion kinetic energy allows us to deduce the inertially confined molecular ion precursor and, therefore, to quantitatively measure and model ionization rates of highly charged ions. Experimentally, this is achieved by placing a window of a box-

car averager around the ion signal for the decay mode of the highly charged ion of interest. Figure 2 shows the number of molecular iodine ions produced as a function of the laser intensity for the decay channels that we have studied. Each point is the average of more than 200 shots, each shot selected to be within a laser energy window whose width is approximately 10% of the average energy. A laser pulse duration of 80 fs was used for these measurements. For comparison purposes we have also measured the first and second ionization states of xenon (not shown in Fig. 2). The xenon data can be used to establish an absolute intensity scale for Fig. 2.

Atomic experiments show that the intensity dependence of the ionization rates can be understood with a slowly varying field approach [7,8]. The ionization potential V_m for $I^{(p-1)+} + I^{q+} \rightarrow I^{p+} + I^{q+}$, where $I^{p+} + I^{q+}$ leads to the products I^{p+} and I^{q+} , is $V_m = V_p + \delta V_{ab} - \delta(\Delta q R E \times \cos(\Theta)/2)$, where V_p is the ionization potential of $I^{(p-1)+}$, δV_{ab} is the change in interaction energy between the ionic constituents of the molecule due to the ionization step in question, Δq is the charge asymmetry, R is the internuclear separation, E is the magnitude of the laser electric field, and Θ is the angle between the dipole and the electric-field direction. We assume that for the zero-field interaction energy of the highly charged ions, V_{ab} is given by the Coulomb interaction for all cases except I_2^+ ($V_m = 9.4$ eV) and I_2^{2+} (inferred [9] ionization potential $V_m = 16.4$ eV). Column 2 of Table I lists the field-free ionization potentials for all observed decay channels.

Using this procedure, we select the ground and charge-transfer states. The energy of these states must be modified to account for the predominant effects of the intense laser electric field. Classically, the modification corresponds to the laser field shifting the interaction po-

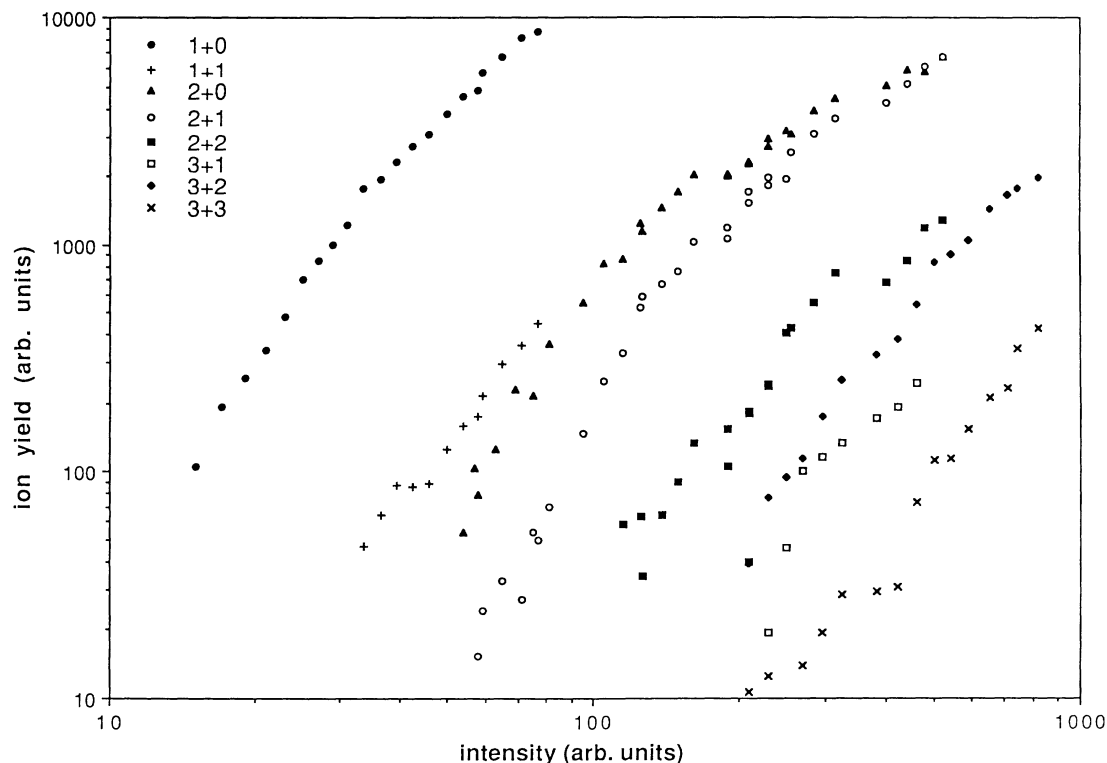


FIG. 2. The ion yield of I_2 as a function of the laser intensity plotted for a number of different charged states. Although plotted in arbitrary units of intensity, we have calibrated the intensity scale using xenon ionization. Ten arbitrary units is approximately $5 \times 10^{12} \text{ W/cm}^2$.

tential of a molecule which has an asymmetric charge distribution by $\Delta q R E \cos(\Theta)/2$, where Δq is the charge asymmetry, R is the internuclear separation, E is the magnitude of the laser electric field, and Θ is the angle between the dipole and the electric-field direction. (These shifts have been analyzed in detail both quantum mechanically and classically for H_2^+ in a dc field [10]. The shifts have been shown [11] to account for the observed strong-field dissociation of the molecular H_2^+ .)

Before analyzing the data in Fig. 2, it is important to recall what is known for atoms. Ionization thresholds can be determined by calculating, when the Coulomb barrier is sufficiently suppressed, that the electron is no longer classically confined. This classical ionization, which agrees with experiment within a factor of 2 when visible radiation is used, has been most thoroughly studied in microwave ionization of Rydberg atom. It is closely related to chaotic electron motion [12].

We use the basic approach of barrier suppression ionization as a guide. Consider a molecular ion as a charged dipole with a dipole moment given by $p = \Delta q R/2$, where R is the internuclear separation. The field distribution of the ionic state is modified by the dipole contribution. In the presence of the combined monopole and dipole field, the usual (atomic) expression for barrier suppression ionization [7] can be used, provided that an effective ionization potential $V_{\text{eff}} = V_m + \Delta q R E \cos(\Theta)/2Z$ replaces the

atomic ionization potential (Z is the ion charge). To derive this expression, we have assumed that the dipole contribution is small. In the limit of a totally charge-asymmetric molecular ion, V_{eff} equals the field-free ionization potential. If V_{ab} is Coulombic, the ionization potential of a single atomic ion is recovered.

All observed channels of molecular decay from a given charge state of I_2^{n+} have nearly the same effective ionization potential in the presence of the laser field (column 3 in Table I). In column 3 we show results for molecules oriented with their dipole moment parallel or antiparallel to the laser field. The effective ionization potentials have been calculated using the experimental threshold fields.

The predicted threshold intensity I_b is presented in column 5 in Table I. The lowest threshold path to a given decay channel is used. We see from the table that the relative threshold laser intensities are very well described by the modified over-the-barrier model. Relative experimental values for ion yield equal to 100 arbitrary units are included in column 4 in the table for comparison purposes. However, if we use the ionization of Xe as an experimental reference intensity [13], the calculated threshold intensities are too large by a factor of approximately 4. For this reason we used an effective dipole moment that is 50% of the actual moment, i.e., $V_{\text{eff}}(E_{\text{cal}}) = V_{\text{eff}}(E_0)$. Otherwise the data presented in the table are completely self-consistent.

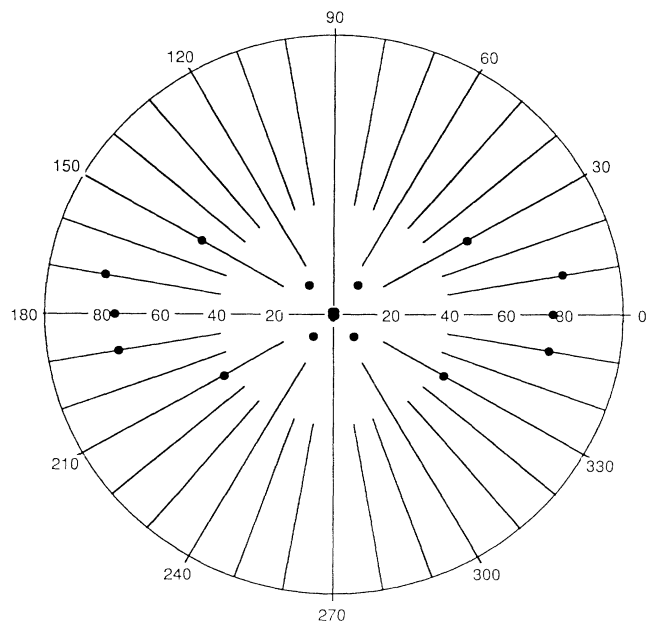


FIG. 3. Angular distribution of ions measured with respect to the laser polarization for decay of $I_2^{3+} \rightarrow I^+ + I_2^+$. I_2^+ ions were observed. Data were taken in only two quadrants. The other two quadrants were obtained by symmetry about the 90° - 270° line.

All data in Figs. 1 and 2 were obtained and analyzed for the laser electric field polarized in the same direction as that of the extraction field in the time-of-flight mass spectrometer. We do not find ion decay products with a large component of their momentum in the direction perpendicular to the laser field. Similar observations are made in long-pulse experiments [14]. Figure 3 shows a typical angular dependence, in this case for the decay channel $I_2^{3+} \rightarrow I_2^+ + I^+$. Higher charge states show an even more pronounced directionality.

There are only two possible explanations for the angular dependence of the trajectory of the decay products of molecular explosions: (1) There is a large difference in intensity required to ionize aligned and nonaligned molecules. Therefore, nonaligned molecules are not ionized. (2) Molecules are given sufficient angular momentum in the direction of alignment during the duration of the laser pulse to effect the subsequent trajectory. The first alternative can be rejected because it is incompatible with the over-the-barrier concepts that are otherwise so successful in explaining the results. That leaves only the second alternative.

The large polarizability of molecular ions provides a possible mechanism for the molecule to gain angular momentum. Since the angular momentum required to account for Fig. 3 corresponds to about ten photons per period, a classical explanation will suffice. Consider an ionic molecule in an electronically excited state corresponding to an asymmetric charge distribution of the final

products. If the field is now varied slowly through 180° , we should expect Δq unit of charge to move rather freely to the energy-degenerate state on the other side of the molecule. This movement of charge corresponds to the coupling of charge-resonant states by the laser electric field [15]. Each atom, therefore, experiences an equal, but oppositely directed impulse, in the direction of the laser polarization for half of the optical cycle. The maximum rotational energy that a molecule receives in the field of a 75-fs pulse of constant intensity ($I = 10^{14}$ W/cm²) and $\Delta q = 1$ corresponds to a quantum number of about $J = 300$. Thus, the angular distribution of the fragments is a measure of the molecular polarizability.

In conclusion, we note a number of important implications: (1) Since high power 10-fs pulses appear technically feasible [3], similar studies are possible for many other inertially confined diatomic or polyatomic molecules. (2) Detailed spectroscopic information of inertially confined molecules can be obtained by improving the energy resolution of the time-of-flight system and by using pump-probe techniques. (3) Plasmas formed from inertially confined molecular ions will be a very nonlinear medium. (4) Transient inversion may occur during the dissociation of highly charged, inertially confined molecular ions because the lifetimes of the charge-symmetric (ground) states will be shorter than that of the charge-asymmetric (excited) states.

- [1] See, e.g., *Atomic and Molecular Processes with Short Intense Laser Pulses*, edited by A. Bandrauk, NATO Advanced Study Institutes, Ser. B, Vol. 171 (Plenum, New York, 1988).
- [2] See, e.g., *Multiphoton Processes*, Proceedings of the Fifth International Conference on Multiphoton Processes, edited by G. Mainfray and P. Agostini (CEA, Saclay, 1991).
- [3] C. Rolland and P. B. Corkum, *J. Opt. Soc. Am. B* **5**, 641 (1988).
- [4] K. Boyer, T. S. Luk, J. C. Solem, and C. K. Rhodes, *Phys. Rev. A* **39**, 1186 (1989).
- [5] L. J. Frasinski, K. Codling, and P. A. Hatherly, *Phys. Lett. A* **142**, 499 (1989).
- [6] R. S. Mulliken, *J. Chem. Phys.* **7**, 20 (1939).
- [7] P. B. Corkum, N. H. Burnett, and F. Brunel, *Phys. Rev. Lett.* **62**, 1259 (1989).
- [8] S. Augst, D. Strickland, D. D. Meyerhofer, S. L. Chin, and J. H. Eberly, *Phys. Rev. Lett.* **63**, 2212 (1989).
- [9] J. H. Beynon, R. M. Caprioli, and J. W. Richardson, *J. Am. Chem. Soc.* **93**, 1852 (1971).
- [10] J. R. Hiskes, *Phys. Rev.* **122**, 1207 (1961).
- [11] G. R. Hanson, *J. Chem. Phys.* **62**, 1161 (1975).
- [12] See, e.g., R. V. Jensen, *Phys. Rev. A* **30**, 386 (1984).
- [13] S. L. Chin, C. Rolland, P. B. Corkum, and P. Kelly, *Phys. Rev. Lett.* **61**, 153 (1988).
- [14] P. A. Hatherly, L. J. Frasinski, K. Codling, A. J. Langley, and W. Shaikh, *J. Phys. B* **23**, L291 (1990).
- [15] P. Dietrich and P. B. Corkum (to be published).